

Object Localization Through a Single Multiple-Model Convolutional Neural Network with a Specific Training Approach

Faraz Lotfi, Farnoosh Faraji, Hamid D. Taghirad

Advanced Robotics and Automated Systems (ARAS), Industrial Control Center of Excellence, Faculty of Electrical Engineering, K. N. Toosi University of Technology, Tehran 1969764499, Iran

Abstract

Object localization has a vital role in any object detector, and therefore, has been the focus of attention by many researchers. In this article, a special training approach is proposed for a light convolutional neural network (CNN) to determine the region of interest (ROI) in an image while effectively reducing the number of probable anchor boxes. Almost all CNN based detectors utilize a fixed input size image, which may yield poor performance when dealing with various object sizes. In this paper, a different CNN structure is proposed taking three different input sizes, to enhance the performance. In order to demonstrate the effectiveness of the proposed method, two common data set are used for training while tracking by localization application is considered to demonstrate its final performance. The promising results indicate the applicability of the presented structure and the training method in practice.

Keywords: Localization, convolutional neural network, training approach, anchor box, image size, single multiple-model, tracking.

*Corresponding author.

E-mail addresses: F.lotfi@email.kntu.ac.ir (F. Lotfi), Taghirad@kntu.ac.ir (H.D. Taghirad).

1. Introduction

Nowadays, several sensors are employed to make a system capable of realizing and handling a critical situation. Computational load and expenses, on the other hand, impose employment of the optimum type and amount of sensors. In an automated robotic system, most of the time a monocular camera may be utilized to provide rich information about the obstacles or intended targets around at a low cost. As a result, object detection through image processing has found its permanent attention among the researches. By introducing new hardware capable of executing deep CNNs, deep learning became the key component of almost all intelligent methods in this field. Unsurprisingly, there is plenty of nominated research works in the field of object detection which is entirely based on CNNs. These approaches may be divided into single and two-stage categories. Single-stage detectors are faster due to having just a single task to localize and recognize objects in an image. Two-stage detectors, however, are reported to be more accurate but not as fast as single-stage ones. Generally, the idea behind these detectors is to perform the detection through two stages. Firstly, an approach is performed to determine and identify the region where the object may highly exist. Then, a classifier window is slid on that region, considering several anchor boxes. A major issue behind these two detectors is the trade-off between speed and accuracy. In this article, this challenging problem has been addressed by suggesting applicable approaches in designing a fast and precise object localizer. Furthermore, to demonstrate its capabilities, a tracking application is considered in which both of the mentioned characteristics become critical in performing perfect object tracking. In what follows, some nominated researches are presented regarding the two mentioned approaches. Then, the key concepts of the proposed object localizer are elaborated.

1.1. Related Works

In the literature, several structures are presented within the single-stage detecting framework such as single-shot multi-box detector (SSD) [1], RetinaNet [2], and you only look once (YOLO) [3]. The latter mentioned method

divides the incoming image into grid cells and uses a specific lost function to perform object detection by processing the image only once. Regarding single-stage detectors, [4] is the earliest convolutional neural networks developed when the hardware was not as powerful as today. This CNN is using three convolutional layers, and one of its main features is, not to connect all the outputs of the second pooling layer to the third convolutional layer. By this means, while the computational cost is reduced, the convolutional filters could learn different features from the data structure.

Another approach has been presented in [5] in which the implementation of *relu* functions instead of *sigmoid* has been proposed as an innovation. This will accelerate the training process and enhance the trainability of the neural network. Furthermore, to improve the results, *overlapping – pooling* has been used instead of the common *pooling* layers. VGG has been proposed as another approach [6], in which by increasing both the layers and the trainable parameters, better outcomes have been reported compared to that of the previous structures. Finally, references [7] and [8] mainly focus on employing different filter sizes such as (1×1) and (5×5) or even (7×7) . Moreover, in [8] non-square filters have been used.

Since objects may appear with various sizes and aspect ratios two-stage detectors will completely scan the image with multi-scale sliding windows. Regarding this concept, region interest CNN (R-CNN) is suggested in [9], resulting in more than 30% improvement in the mean average precision (mAP) of the results. In R-CNN by using selective search approach [10], $2k$ proposal regions are applied to accurately and quickly search an image, which reduces the search space. Furthermore, feature vectors will be extracted for each region by a CNN, and positive and negative scores (for objects and background) will be set with a pre-trained linear SVM. By this means the required bounding box is determined for classification.

R-CNN resizes the images into proposal regions with a fixed size since fully-connected (FC) layers require fixed-size images for processing. This may yield unpleasant geometric distortions. To remedy this problem, SPP-Nets are devel-

oped with a different architecture to handle the issue [11]. Needing large storage while processing the whole image with SPP-Net, fast R-CNN produces a feature map that helps to gather one fixed-length feature vector for each region. As it is remarked, the feature vectors are applied to estimate both the bounding box locations and the related class [12] (it includes C classes for the objects and one class for the background). Regarding the region proposal computation, region proposal network (RPN) is introduced in faster R-CNN approach [13]. In this network, the convolutional features will be shared with the detector to significantly reduce the training time. Despite the accuracy and high speed of the faster R-CNN, it faces various problems while dealing with small scale objects in the images. For instance, it has major limitations over the COCO data set [14], which contains a wide range of objects on different scales. To handle this major problem combination of complementary information of multiple sources has been suggested in the literature [15, 16, 17].

1.2. The Key Concepts

The bottleneck of the above-mentioned approaches is the number of the necessary anchor boxes in terms of the computational cost. Thus, one way to enhance the performance of such detectors is to identify the ROI as accurately as possible and to determine the center point of the object bounding box precisely. Furthermore, needing a specific output size, almost all the detectors use a fixed size image as the input. This will reduce the performance and demands a deeper structure for more various sizes. As a representative, even for YOLOv3 as a strong approach applicable to a wide range of applications, it has been suggested to change the structure and anchor boxes to detect small objects or specific ones more accurately. Considering this drawback, it is essential to have a flexible structure for a general-purpose network, to detect a wide range of objects in different sizes. Of course, it is challenging to properly train such a neural network; thus, a complete framework may be very beneficial to be presented to further make it easier for the researchers to design and test their own structures.

The main contribution of this paper is firstly, to propose a new approach in training deep CNNs to precisely localize objects in an image. Secondly, a single multiple-model is presented to handle the object localization for a wide range of object sizes without the need for changing the neural network input size. The code has been implemented such that, it would be easy to develop further structures. Moreover, in this paper, all the underlying concepts mentioned in the previous researches are used to increase the performance of the proposed network. The outcome of this research can be used either for a two-stage detector in multi-object detection or a single object detector individually. Moreover, to demonstrate the effectiveness of the suggested approach, a tracking application has been considered where the proposed tracker is compared to the eight commonly used OpenCV trackers [18]. As a result, the performance of the suggested tracker is closely comparable to the others and better in some situations.

The rest of this article is organized as follows. In the second section, the structure will be presented in detail, and the challenges are remarked together with their suggested solutions. In section three, the method for the training process will be elaborated as well as the issue of producing the desired data set. Section four focuses on the results and performance analysis. Finally, the concluding remarks are given in the last section.

2. The Proposed Structure

This section describes the proposed architecture of the network used for diverse input sizes. As it has been mentioned before, this structure is different from the commonly presented ones, capable of handling three various input sizes. When an image enters the network as the input, according to its size it will be processed through the specific convolutional layers to produce the output. Unlike common CNN architectures, the image will not penetrate all the layers of the network, and this structure can handle multiple models inside a single convolutional model. By this means, there is no need to change the structure

of the network to deal with small or large objects. Two important notes are to be considered here. The output size has to be fixed to avoid problems in the training process, therefore, we considered three different image sizes in this paper. Furthermore, it is beneficial to have common layers between the three models. This will reduce the number of required trained variables, and lead to an optimized structure. This method is much more beneficial than using multiple distinct models.

Regarding the aforementioned points, a flexible structure consisting of both distinct and common convolutional layers is suggested in this paper as illustrated in Fig. 1. As it can be seen in this figure, three inputs of $(448, 448)$, $(224, 224)$, and $(56, 56)$ are considered for the network. For each input image, considering the closest size, the corresponding distinct convolutional layers will be processed through. The main underlying idea here is to downsample the image while not losing indispensable information. In this network for an input image with size over $(336, 336)$, the green blocks branch of the CNN will be activated, while both the blue and the red branches became inactive. Furthermore, the yellow and the black branches perform the processing to result in the desired output. Note that, the black branch is common, and in terms of using convolutional layers, the longest among all the layers. Since having long enough common layers is necessary to reach the required performance. There are two outputs for the network, namely the ROI and center point matrices to be used in training this structure whose details are presented in the next section. Note that the "Max" notation used in the blocks represent the max-pooling layers following the convolutional ones.

Remark 1: There are convolutional layers with $(2, 2)$ sizes and $(2, 2)$ strides. These are responsible to perform something more than just max-pooling. However, max-pooling layers may be used, while slightly reducing the performance.

Remark 2: In the common layers, max-pooling layers are used rather than convolutional ones with $(2, 2)$ strides. This is mainly considered to reduce both the number of trainable variables and structural complexity.

The presented structure represents the main idea behind having multiple

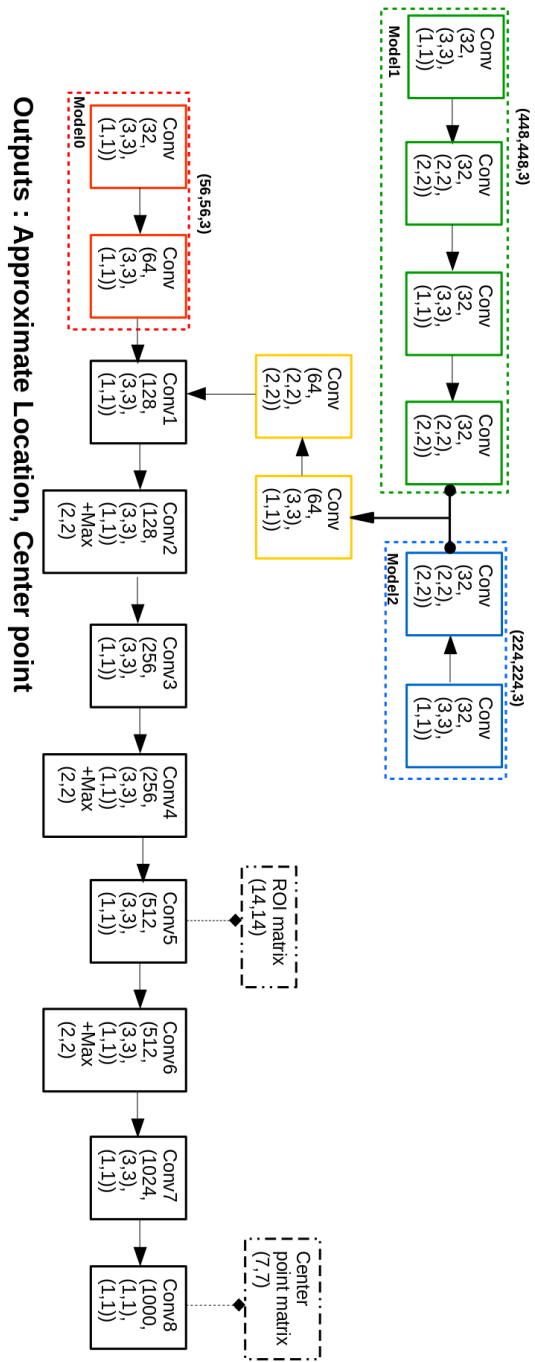


Figure 1: The proposed flexible structure.

models in a single convolutional model. Depending on the application, one may extend this structure to have more distinct branches performing specific processing on inputs with different sizes. Hence, the proposed structure can be employed for other image processing purposes, by adjusting the loss function used for the optimization.

3. The Training Approach

In this section, an effective approach is presented to train a neural network for object localization. The main purpose of the proposed convolutional neural network is to precisely identify an ROI and the center point of the object. Considering the underlying concepts used for effective training, some methods have been tested and evaluated to enable such a light CNN in terms of accuracy and speed, perform well in practice.

3.1. The Concept

Taking the structure presented in section 2, there are some challenges in training the distinct layers. In fact, except for the common black branch which is always active for all the input sizes, the gradient has to be backpropagated only to the corresponding activated layers. It is undeniable that those inactive layers will have a zero gradient for the irrelevant input. When it comes to the implementation, however, it would be challenging to count no gradient support for those layers. This issue has been solved by considering distinct trainable variables in the training process. For each input image, just the trainable variables of the corresponding activated layers and the common layers are updated, and the other passive layers will remain unchanged. By this means, a training process could be implemented for such flexible structures. In the implemented code the training is performed differently for various image sizes.

As Fig. 1 shows, the arrangement of the features in the feature maps are not changed through the layers. Therefore, an object in a specific location will trigger the same place of the feature maps as the image is processed. By using



Figure 2: A sample image for describing the training concept.

this key concept, it is possible to train the CNN by representing the object location with a location matrix. This is similar to considering a mask for each image. However, these masks are different from those used in segmentation applications like [19]. To clarify, here there is no need to classify each pixel in the image, and it is sufficient to assign the pixels belonging to the corresponding object. This is done by taking a matrix with binary values, whose one elements correspond to the place where the object exists. In the following example, this idea is visualized. Consider Fig. 2 as the incoming image, and divide it into a (14×14) grid. Take a (14×14) matrix, whose component is equal to one if a part of the object is located at that position, and zero if not. As a result, the

following matrix is obtained.

$$\begin{bmatrix}
 0 & 0 & 0 & 0 & 0 & 0 & 0 & 0 & 0 & 0 & 0 & 0 & 0 & 0 & 0 \\
 0 & 0 & 0 & 0 & 0 & 0 & 0 & 0 & 0 & 0 & 0 & 0 & 0 & 0 & 0 \\
 0 & 0 & 0 & 0 & 0 & 0 & 0 & 0 & 0 & 0 & 0 & 0 & 0 & 0 & 0 \\
 0 & 0 & 0 & 0 & 0 & 0 & 0 & 0 & 0 & 0 & 0 & 0 & 0 & 0 & 0 \\
 0 & 0 & 0 & 0 & 1 & 1 & 1 & 1 & 1 & 1 & 1 & 1 & 1 & 0 & 0 \\
 0 & 0 & 0 & 0 & 1 & 1 & 1 & 1 & 1 & 1 & 1 & 1 & 1 & 0 & 0 \\
 0 & 0 & 0 & 0 & 1 & 1 & 1 & 1 & 1 & 1 & 1 & 1 & 1 & 0 & 0 \\
 0 & 0 & 0 & 0 & 1 & 1 & 1 & 1 & 1 & 1 & 1 & 1 & 1 & 0 & 0 \\
 0 & 0 & 0 & 0 & 1 & 1 & 1 & 1 & 1 & 1 & 1 & 1 & 1 & 0 & 0 \\
 0 & 0 & 0 & 0 & 1 & 1 & 1 & 1 & 1 & 1 & 1 & 1 & 1 & 0 & 0 \\
 0 & 0 & 0 & 0 & 1 & 1 & 1 & 1 & 1 & 1 & 1 & 1 & 1 & 0 & 0 \\
 0 & 0 & 0 & 0 & 1 & 1 & 1 & 1 & 1 & 1 & 1 & 1 & 1 & 0 & 0 \\
 0 & 0 & 0 & 0 & 0 & 0 & 0 & 0 & 0 & 0 & 0 & 0 & 0 & 0 & 0 \\
 0 & 0 & 0 & 0 & 0 & 0 & 0 & 0 & 0 & 0 & 0 & 0 & 0 & 0 & 0
 \end{bmatrix} \tag{1}$$

Now dividing the image into a (7×7) grid. Similarly, the corresponding (7×7) matrix can be defined to identify the object center point as follows.

$$\begin{bmatrix}
 0 & 0 & 0 & 0 & 0 & 0 & 0 \\
 0 & 0 & 0 & 0 & 0 & 0 & 0 \\
 0 & 0 & 0 & 0 & 0 & 0 & 0 \\
 0 & 0 & 0 & 0 & 0 & 0 & 0 \\
 0 & 0 & 0 & 0 & 1 & 0 & 0 \\
 0 & 0 & 0 & 0 & 0 & 0 & 0 \\
 0 & 0 & 0 & 0 & 0 & 0 & 0
 \end{bmatrix} \tag{2}$$

A point to ponder is, to obtain the ROI, one may utilize other matrices (e.g. (28×28) or (16×16)) rather than the exact (14×14) matrix. The important thing is to utilize the output of a convolutional layer in Fig. 1 which results in a better outcome. Taking this structure into consideration, the corresponding proper choice is the (14×14) matrix. This is because of two reasons; First, down-sampling yields richer information, and second, more convolutional layers

result in a more flexible structure. Furthermore, to employ such a matrix in determining the ROI, post-processing is necessary which makes a smaller matrix with richer features, a better choice in terms of both the accuracy and the speed. On the other hand, the use of the second (7×7) matrix is important in preventing failures in certain situations. This point is covered in the experimental results section in more detail. This matrix helps to get more robust results, and furthermore, it produces another gradient flow which makes the (14×14) matrix more oriented towards the object location. The same point mentioned about utilizing other matrices rather than the exact (14×14) is valid about the (7×7) matrix, as well. Taking these two matrices as ground truth, the following loss function is defined:

$$L = \alpha_1(\sum(\gamma^{2(\hat{p}_1-p_1)})) + \alpha_2(\sum(\gamma^{2(\hat{p}_2-p_2)})) \quad (3)$$

where p_1 and p_2 are the true values of (14×14) and (7×7) matrices, and \hat{p}_1 and \hat{p}_2 are their estimats obtained by the CNN, respectively.

Remark 3: α_1 and α_2 are the coefficients used to compensate for the bias in each term, and γ is a positive value less than one ($0 < \gamma < 1$).

Remark 4: Note that the matrices \hat{p}_1 and \hat{p}_2 are obtained by using an average over the feature-maps followed by the "softmax" function.

As it can be seen, equation (3) contains two terms, each one corresponding to the relating matrix. The first term is responsible for determining the object's ROI. This will result the CNN to generate a matrix in which lae larger component of the matrix correspond to higher probability of existence of a part of object in that component. The second term is used for identifying the object center point in which the (7×7) matrix is utilized. Note that, utilizing few layers to get the (7×7) matrix from the (14×14) matrix by down-sampling effectively reduces the number of probable anchor boxes when this CNN is employed in a two-stage detector.

Remark 5: Comparing the proposed loss function to commonly used mean square error one, it has the advantage of magnifying the importance of the error



Figure 3: A sample image from the NFS dataset

in the components related to the object location. By this means, the necessity of finding which components may contain a part of an object is well addressed.

3.2. The Dataset

At this stage, let us elaborate on the proper dataset used to train the proposed network. Reconsider loss function (3), where for each image, the two (14×14) and (7×7) matrices shall be produced. Taking into consideration the fact that the existing annotations often contain bounding boxes, it is very simple to get the required matrices via them. Since a single object tracking application is taken to further illustrate the power of both the proposed training approach and the flexible structure, a dataset called "NFS" [20] is used, which is known as an object tracking benchmark. Necessary modifications are performed on this dataset to produce the required data.

To describe the process, consider Fig. 3 as the main image. Since in the tracking application at the first frame the user determines the requested object to be tracked, it can be assumed that the approximate object location is given. Therefore, it is rational to process just a part of the image rather than the whole image. In this regard, Fig. 4 indicates the relevant part of the image which will be used as input to train the network. Note that, here the object



Figure 4: The cropped part which is used as the CNN input for the tracking application

may be located in the image center, however, in the next frame, as there is no information about where the object is, the same part of the image is a proper choice to be used. Apparently, this time the object is not located at the center since it has moved from its previous location. Hence, in order to be capable of detecting the object in any location of the input image, it is better to randomly locate objects in various places. To further illustrate this important point, in Fig. 5 some representative samples of the produced dataset is shown. It can be seen that the objects are not located at the center, different object types are considered, while the images have various sizes.

Remark 6: A point to ponder is that the annotations of the NFS dataset have to be changed according to the new images indicated in Fig. 5.

4. Experimental Results

In this section, the results of training the proposed structure illustrated in Fig. 1 on the produced dataset are reported. The training approach is the same as suggested in the previous section in which $\alpha_1 = 10^{-5}$, $\alpha_2 = 234$, and $\gamma = 0.0001$ are used. The optimizer used to train the CNN is the stochastic gradient descent (SGD) with 0.001 learning rate, and the CNN has been trained for about 65 epochs. Furthermore, to avoid having any bias in the dataset, about 8700 frames are selected in which there are approximately 500 images for each object type. Considering different object types, the input images will have various sizes activating different branches of the proposed structure. In what follows, first, some test images with different sizes will be processed and the CNN outputs are investigated. Second, a study is reported on the possibility of

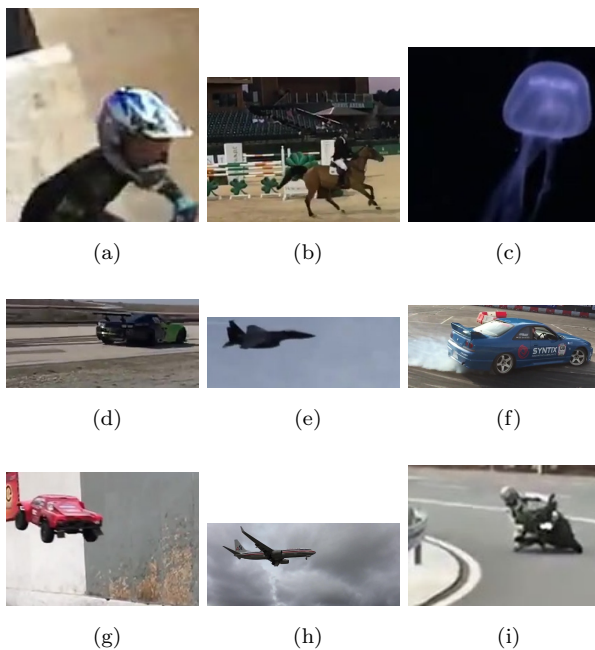


Figure 5: Some representative samples of the produced dataset

using higher resolution ROI matrices such as (28×28) . Then, the trained CNN is employed as a single object tracker considering three scenarios. Several challenges in the implementation are addressed. To evaluate the proposed tracker, the results are compared to some commonly used trackers such as GOTURN and other OpenCV trackers with respect to a common measure. Finally, to further demonstrate the proposed approach capabilities, the tracker is trained on another dataset called LaSOT[21] and it is compared to a recently presented tracker to analyze its performance in more detail.

4.1. Results on Images with Various Sizes

First, let's investigate the performance and the details of the algorithm through an image. Thereafter, various image sizes are processed to further demonstrate the applicability of both the suggested structure and the proposed training method. Reconsider Fig. 2 which has been classified to the (448×448) size. Taking this image as the CNN input, the output for the (14×14) matrix

is obtained as:

$$\begin{bmatrix}
 0.06 & 0.07 & 0.07 & 0.07 & 0.07 & 0.07 & 0.07 & 0.07 & 0.07 & 0.07 & 0.07 & 0.07 & 0.07 & 0.06 \\
 0.06 & 0.07 & 0.07 & 0.07 & 0.07 & 0.07 & 0.07 & 0.07 & 0.07 & 0.07 & 0.07 & 0.07 & 0.07 & 0.06 \\
 0.06 & 0.07 & 0.07 & 0.07 & 0.07 & 0.07 & 0.07 & 0.07 & 0.07 & 0.07 & 0.07 & 0.07 & 0.07 & 0.06 \\
 0.06 & 0.06 & 0.07 & 0.07 & 0.07 & 0.07 & 0.07 & 0.07 & 0.07 & 0.07 & 0.07 & 0.07 & 0.06 & 0.06 \\
 0.06 & 0.06 & 0.06 & 0.07 & 0.07 & 0.08 & 0.08 & 0.07 & 0.06 & 0.06 & 0.06 & 0.06 & 0.06 & 0.06 \\
 0.05 & 0.05 & 0.06 & 0.06 & 0.07 & 0.09 & 0.09 & 0.08 & 0.07 & 0.07 & 0.06 & 0.06 & 0.06 & 0.05 \\
 0.05 & 0.05 & 0.05 & 0.06 & 0.07 & 0.09 & 0.10 & 0.09 & 0.08 & 0.07 & 0.07 & 0.06 & 0.05 & 0.05 \\
 0.04 & 0.04 & 0.04 & 0.05 & 0.07 & 0.09 & 0.11 & 0.10 & 0.09 & 0.08 & 0.07 & 0.06 & 0.04 & 0.04 \\
 0.04 & 0.04 & 0.04 & 0.052 & 0.06 & 0.09 & 0.11 & 0.11 & 0.10 & 0.09 & 0.07 & 0.05 & 0.04 & 0.04 \\
 0.04 & 0.04 & 0.04 & 0.05 & 0.06 & 0.08 & 0.10 & 0.11 & 0.11 & 0.09 & 0.07 & 0.06 & 0.05 & 0.04 \\
 0.05 & 0.05 & 0.05 & 0.05 & 0.06 & 0.07 & 0.09 & 0.101 & 0.10 & 0.092 & 0.07 & 0.06 & 0.05 & 0.05 \\
 0.06 & 0.06 & 0.06 & 0.06 & 0.06 & 0.07 & 0.07 & 0.08 & 0.08 & 0.08 & 0.07 & 0.06 & 0.06 & 0.05 \\
 0.06 & 0.07 & 0.07 & 0.07 & 0.06 & 0.07 & 0.07 & 0.07 & 0.07 & 0.07 & 0.07 & 0.07 & 0.06 & 0.06 \\
 0.07 & 0.07 & 0.07 & 0.07 & 0.07 & 0.07 & 0.07 & 0.07 & 0.07 & 0.07 & 0.07 & 0.07 & 0.06 & 0.06
 \end{bmatrix}$$

(4)

It is easy to identify a proper threshold by solving an optimization problem over the test dataset to maximize the overlap between the object location and the components in the (14×14) matrix. Here, the threshold is set to 0.09 by which the ROI will be accurately determined. Fig. 6a indicates a visual outcome of using this threshold on the (14×14) matrix in which the red-colored parts represent the matrix components with values higher than 0.09. As it can be seen, the result is promising and the location of the object has been precisely identified. Now, let's check the (7×7) matrix as it is responsible for presenting probable center point candidates:

$$\begin{bmatrix}
 0.14285 & 0.14285 & 0.14285 & 0.14285 & 0.14285 & 0.14285 & 0.14285 \\
 0.14285 & 0.14285 & 0.14285 & 0.14285 & 0.14285 & 0.14285 & 0.14285 \\
 0.14282 & 0.14282 & 0.14282 & 0.14303 & 0.14282 & 0.14282 & 0.14282 \\
 0.11155 & 0.11155 & 0.14936 & 0.22829 & 0.17611 & 0.11155 & 0.11155 \\
 0.10102 & 0.10102 & 0.13884 & 0.24611 & 0.2102 & 0.10171 & 0.10102 \\
 0.13189 & 0.13189 & 0.13189 & 0.17523 & 0.16529 & 0.13189 & 0.13189 \\
 0.14285 & 0.14285 & 0.14285 & 0.14285 & 0.14285 & 0.14285 & 0.14285
 \end{bmatrix}$$

(5)

Similarly, it is easy to find an appropriate threshold which is set as 0.18 in here. Fig. 6b illustrates the outcome of using this threshold, in which, the matrix components higher than 0.18 are displayed with the green-colored pixels. Utilizing these two matrices, the ROI along with the probable center points of the object are found. However, the problem of the computational cost is

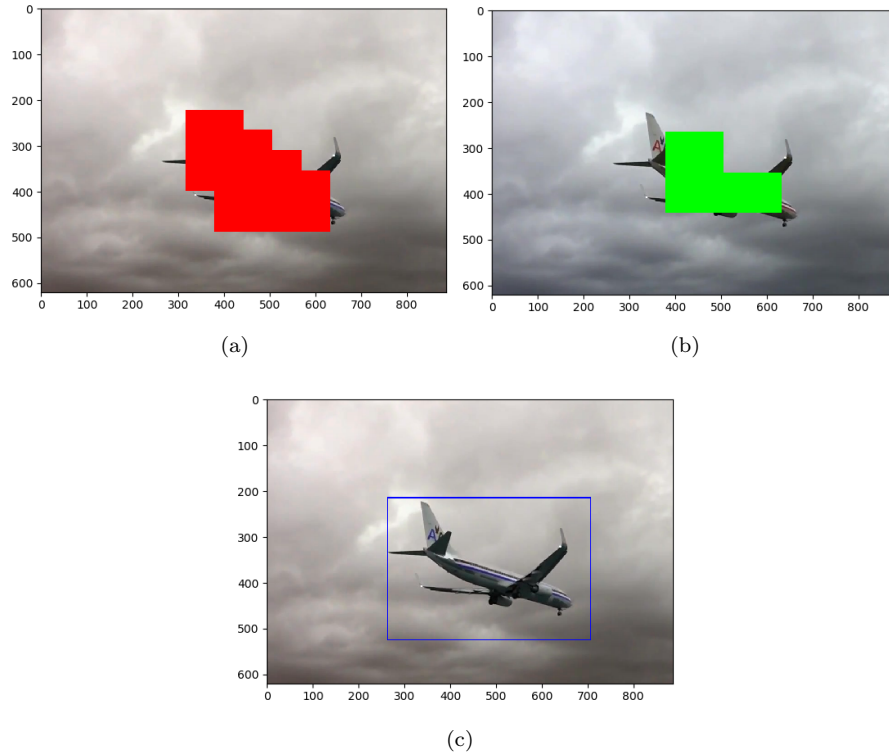


Figure 6: Visual outcomes of the ROI matrix alongside the center matrix, and the fitted bounding box

predominant. Thus, the easiest way of searching for the values higher than the determined thresholds might not be proper computational-wise. In this regard, a specific function "max pool with argmax()" is used on the (14×14) matrix to find the larger values than the threshold and their arguments. Thereby, instead of searching through (14×14) components, values higher than the threshold are found quite quickly. Having these arguments, it is possible to modify the bounding box scale. The higher the values over the threshold, the higher the scale. Next, for the (7×7) matrix the same approach is used to identify the candidates, and the mean value of them will be utilized as the final center point for the bounding box.

In object tracking the target is to locate the object at each frame. Having

some information from the initial frame, it is possible to modify and shift the initial bounding box by the two (14×14) and (7×7) matrices. Of course, there are other ways to implement such an algorithm; however, since the speed is of high importance, it has been tried to use nearly the fastest approach. Fig. 6c indicates the most probable bounding box for the object. To demonstrate the applicability of the proposed structure, some other images with various sizes are tested and the results are reported in Fig. 7. In this figure three rows are presented which illustrate the visual outcomes of the ROI matrix, the center point matrix, and the most probable bounding boxes, respectively. Among over 350 test images the average intersection over union (IoU) is about 0.75 which verifies the effectiveness of the proposed approach. Furthermore, Fig. 8 shows the IoU obtained from processing lots of images with various sizes. In this figure, three lines represent the results of each of the three mentioned models. As it is seen, results are promising and the suggested CNN has uniformly suitable performance on various image sizes.

4.2. A Study on a Higher Resolution ROI Matrix

In this part of the article, the possibility of using a higher resolution ROI matrix is studied. In this respect, the proposed architecture is modified and reduced with less convolutional layers to output a (28×28) matrix. Then, it is trained on the NFS dataset for 100 epochs. Note, in the reduced structure the convolutional layers are reduced and the problem complexity on the other hand, has been increased due to the higher resolution of the input image. In order to have a fair comparison between the two results, a metric is used on a test set which counts the $L1$ norm of the error between an output and the given ground truth. Furthermore, since the proposed architecture has three branches, there are three outcomes corresponding to the three models in the report. To get better comparison the (14×14) matrix is resized to a (28×28) one, such that it could be directly compared to that of the other approach that uses the (28×28) matrix. By comparing the results given in Fig. 9, it is clear that the outcomes

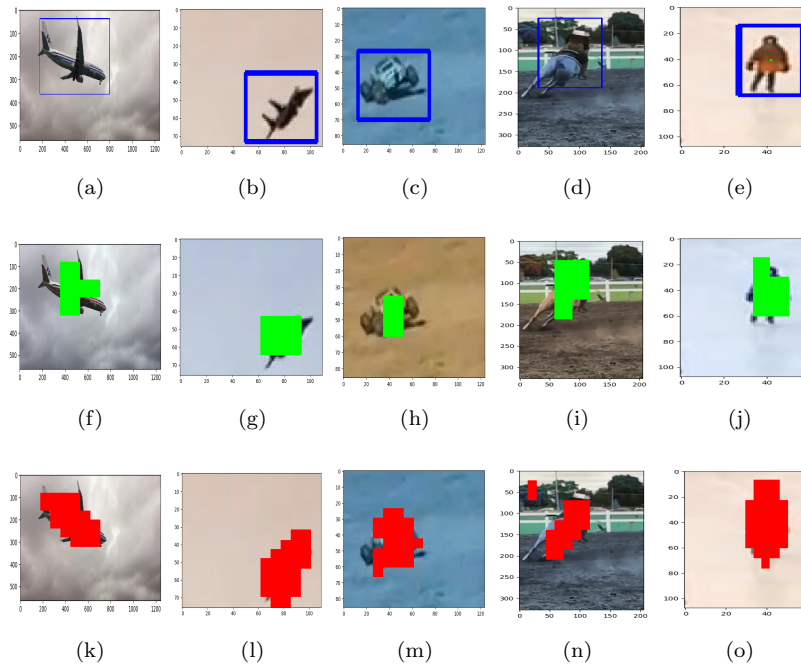


Figure 7: Some samples of the test results.

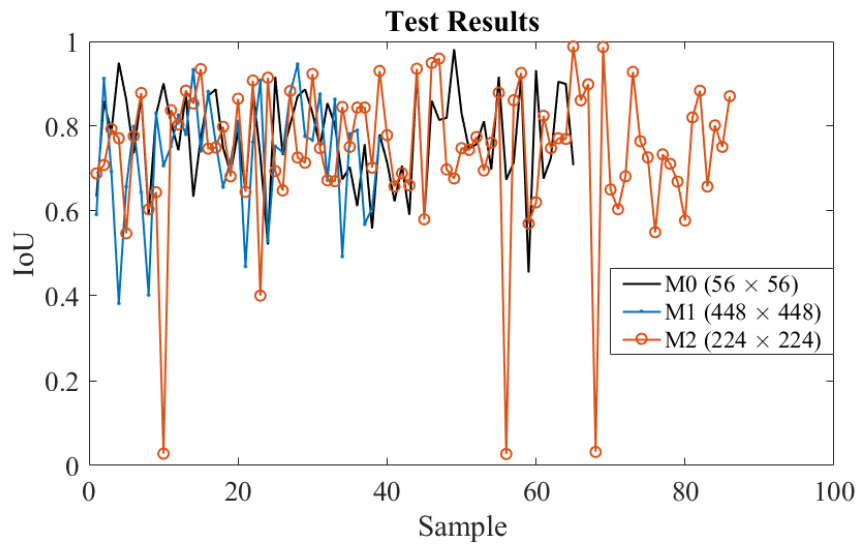


Figure 8: IoU for several test images considering various sizes.

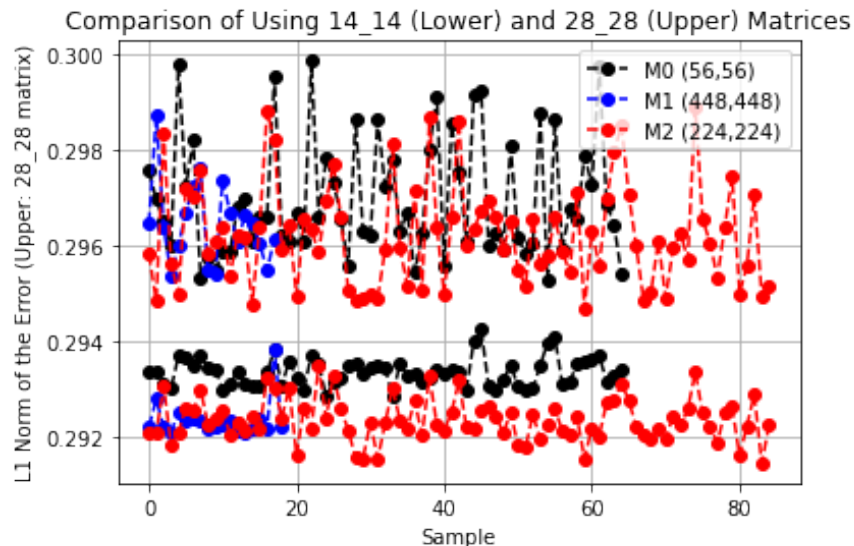


Figure 9: Results of employing the presented approach and a reduced architecture with higher resolution.

of utilizing the presented architecture are more reliable in all the three models while the accuracy is higher. As a consequence, it is readily possible to employ a higher resolution matrix. However, considering all the details presented in this section, it is proposed to use the (14×14) matrix in practice.

4.3. Results of the Proposed Tracker

Now that the performance of the CNN on individual images is verified, some tracking scenarios are presented by which a comparative study over eight other trackers is reported, and the performance of the proposed tracking algorithm is evaluated. The purpose of considering these scenarios is to evaluate the results of the suggested approach in both estimating center points and identifying the object scale. The IoU at each frame is considered as a metric of the tracker performance. Note that, the only limitation here in tracking, is to always have the object in the camera field of view. Before reporting the results, a brief description of each tracker is presented to further get insight to their characteristics. The first tracker used is called Boosting, one of the oldest trackers which

has a significant performance in detections; however, since it is too slow, it can be utilized only as a tool for comparing the other designed trackers [22]. Multi instance learning (MIL) tracker leads to a robust tracking compared to that of the other traditional trackers. Although this tracker is more accurate than the Boosting tracker, it faces more problems to accurately report the failures [23]. The other tracker is the kernelized correlation filter (KCF) which operates faster than MIL and Boosting trackers but it may not handle the occlusion [24]. Dealing with tracking the occluded objects, channel and spatial reliability tracker (CSRT) operates more efficiently, with the expense of being slower in computation [25]. Medianflow tracker has been proposed to particularly track small and low-contrast objects [26]. However, it fails to track fast-moving objects and also the objects with quick changes in the appearance. This tracker, however, reports the failures very accurately. It also tracks the object in both forward and backward directions which reduces the error significantly. In the tracking-learning-detection (TLD), the tracker follows the detected object at each frame, the detector localize observed features and the learning module is responsible to reduce the error in the future frames [27]. The high speed MOSSE tracker, is reported to be robust against variations in lighting, scale, pose, and nonrigid deformations [28]. Finally, the only CNN based tracker here, GOTURN [29] utilizes two frames to track the object while employing a special structure.

Fig. 10 illustrates the first experiment scenario in which there is a car drifting over the road and the challenge is to keep the IoU high, while the object is becoming larger in the image. In all the reported scenarios the moving trajectory of the object is illustrated by the colored bounding boxes. To compare the proposed tracker with the others, the IoU is determined at each frame, and the results are reported in two diagrams to quantitatively compare the performance of the trackers. Fig. 11 indicates the results obtained from various trackers in this experiment. As it is seen in this figure, despite the low IoU at the beginning, the proposed tracker has almost constant performance regardless of the object changing size. On the other hand, other trackers perform poorly as the object size begins to change quickly. Note that the fluctuations seen in the IoU of the

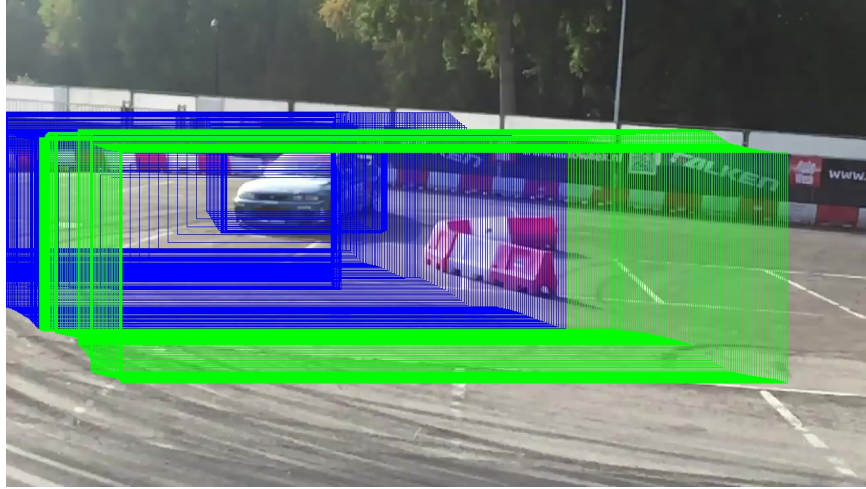


Figure 10: The first scenario (A drifting car). The colored bounding boxes indicate the motion trajectory.

proposed approach, indicate that the tracker is trying to modify the bounding box to keep the IoU as high as possible.

The second experiment scenario is shown in Fig. 12 in which a car is moving towards the camera while due to its far distance it has a relatively small size in the image. Here the challenge is different from the previous scenario, in the sense that the object size is much smaller while there is a shift in the object center point to be estimated precisely. This is due to the fact that a small error in the center point may result in poor performance or even losing the object features in practice. Note that in this scenario the camera moves as well. The results of using the trackers are reported in Fig. 13. As shown in Fig. 13a, the performance of the proposed tracker is almost better everywhere. In here the GOTURN tracker has failed to perform well, and compared to the conventional methods, MEDIANFLOW tracker performs the best. This result deserves more attention since it highlights the fact that CNN based trackers such as GOTURN may perform poor in scenarios like this while the MEDIANFLOW could possibly yield a better outcome. However, the proposed tracker has performed significantly better than the best of other trackers.

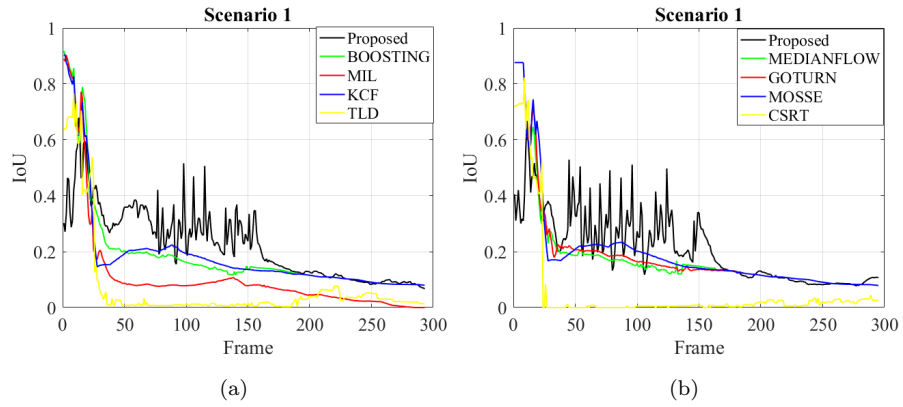


Figure 11: Results of the trackers for the first scenario. Each tracker's outcomes are given with a specific colored-line and the proposed tracker has been shown by the black line in both figures.



Figure 12: The second scenario (a far away car).

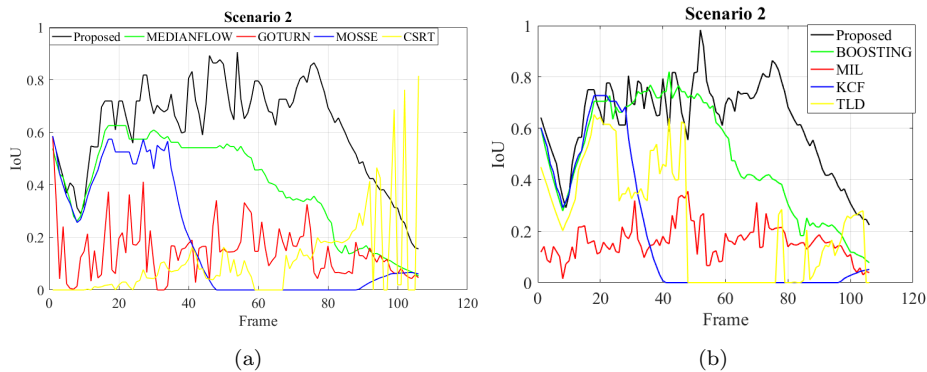


Figure 13: Results of the trackers for the second scenario

Finally, in the last experiment scenario, the purpose is to evaluate the proposed tracker in long term tracking while the object center point significantly varies in both directions. As it can be seen in Fig. 14, a red disk moves through the blue, the green, and the red bounding boxes, respectively. These boxes illustrate the location of the disk in the next frames. Furthermore, the color of the boxes is changed whenever it comes to a hit. Note that the game tools are quite similar to the red disk which may yield failure when it comes to a hit. This will help to explain why both the (14×14) and (7×7) matrices are needed. In fact, considering the information obtained from the (14×14) matrix, one may think that utilizing this matrix, it is possible to estimate the center point, as well. However, in cases like such experiment, when the tracked object get close to another similar object in the same region, using only the (14×14) matrix will result in failure. This is because utilizing the single (14×14) matrix may result in false outcomes since there are some other objects or surfaces in the environment which may seem just like a part of the object. As a result, employing this matrix to obtain the center point will result in errors in situations like this.

Fig. 15 indicates the performance of the trackers in detail. In Fig. 15a it can be seen that although the BOOSTING tracker has performed well before its failure it could not distinguish the red disk with the red game tool at the second

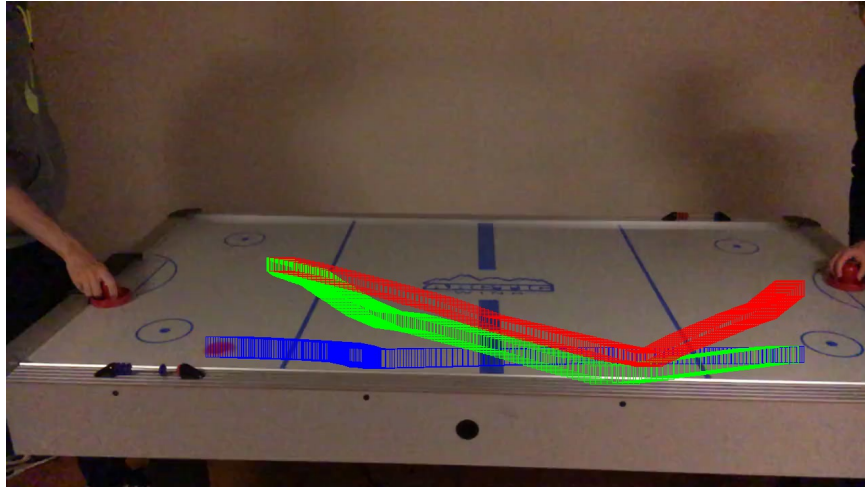


Figure 14: The third scenario (a red disk).

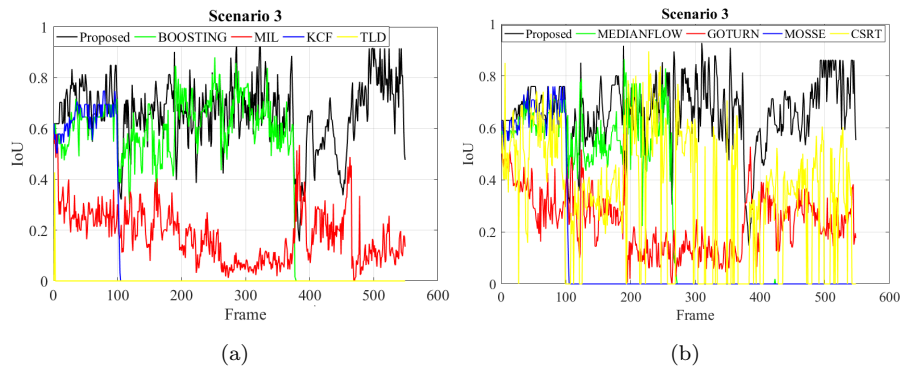


Figure 15: Results of the trackers for the third scenario

contact point. Regarding the results, both the proposed tracker and the MIL tracker has accomplished the task. However, the results of the proposed tracker are far better in terms of IoU measure. Fig. 15b illustrates the functionality of the other trackers. As it is seen in this figure, the MEDIANFLOW tracker has performed just like the BOOSTING, however, it has failed at the same occasion. In this result, there are three trackers capable of tracking the object during the whole experiment, while the proposed tracker has the best performance. Although the CSRT tracker did not fail and it has accomplished the task, it has very large fluctuations that downgrade its functionality, and maybe the GOTURN's performance is more desirable in practice.

Notice that one important aspect of a tracker is its speed. Considering the light structure of the proposed tracker by using a 1650 NVIDIA GeForce GPU, the minimum speed of this tracker is 40 FPS for images with size (448×448) , while it rushes to 120 FPS for (56×56) image size. Although a single object tracking application is studied here, the proposed tracker may be used for multiple-object tracking tasks. It is possible to track several objects by adding an adequate number of trackers since the suggested tracker has been implemented as an object in the code. The speed of the proposed tracker is given in Table. 1 for further analysis. This table illustrates the maximum speeds of the employed trackers obtained on the same hardware. As it is seen in this table, the maximum speed of the proposed tracker is 120 FPS, which is clearly much better than that of conventional trackers. Furthermore, comparing to the two trackers with higher running speed than that of the proposed tracker, the superiority in performance justifies the use of the proposed tracker which is definitely implementable in real time applications.

4.4. *The Failure Analysis*

Considering the high importance of failure rates among trackers, in this subsection, a monte-carlo simulation has been studied to further investigate the proposed tracker performance. Since almost all of the trackers are highly sensitive to the initialization, each scenario is repeated for 10 times taking different

Table 1: This table reports the speeds of the trackers each obtained by running the corresponding tracker several times in a simple tracking task and saving the best running time. Note, in the mentioned task a small object is considered to be tracked to further help some of the trackers to be faster.

Tracker	Proposed	BOOSTING	MIL	KCF	TLD	MF	GOTURN	MOSSE	CSRT
Max Speed (fps)	120	25	12	35	10	87	100	800	23

initial conditions for the trackers. Not only does this take various initializations into account but also it may challenge the probable randomness in the trackers. In the beginning for the first time, the initialization is performed manually. Then, for the rest of the 9 simulations, this initial condition is changed stochastically while considering a limited bound of randomness. Moreover, each scenario has been divided into three or four parts each of which is associated with a specific challenging task such as a fast movement, an occlusion, or a big change in the object size. Note that except for the last scenario, the results in the previous section are given for a part of a video. The whole videos, however, have been taken in this subsection to further consider various challenges such as camera movement.

To illustrate the results, Table 2 is presented in which each row shows the results of a simulation. Furthermore, the three numbers in each element present the corresponding scenario result in that simulation (e.g. in $(0, 2, 1)$, 2 stands for the number of failures in the second scenario in the corresponding simulation). Before getting into the detail of the results, let’s investigate the challenges in each scenario first. The first scenario has been divided into four parts including various object views, changing in the object size, shaking camera, and cluttered background. The second scenario is associated with various object sizes while having different object views, moving camera, fast movement while becoming small quickly, and a short-term full occlusion. Finally, the third scenario challenges are the moments in which the disk is hit by the player. In contrast to the other two scenarios, three failure points are considered in this scenario since

Table 2: Results of the monte-carlo simulation given to further analyze the proposed tracker in different situations while taking failure rates into consideration

Proposed	BOOSTING	MIL	KCF	TLD	MF	GOTURN	MOSSE	CSRT
(0,0,1)	(0,2,1)	(0,1,1)	(0,4,3)	(0,4,3)	(0,2,0)	(0,3,3)	(0,4,3)	(2,4,3)
(0,1,1)	(0,2,0)	(1,2,2)	(0,4,3)	(0,3,3)	(0,2,1)	(0,1,1)	(0,4,3)	(4,3,3)
(0,2,1)	(0,3,1)	(0,2,2)	(0,3,3)	(0,4,3)	(0,2,1)	(0,1,3)	(0,3,3)	(1,3,3)
(0,1,3)	(0,2,1)	(0,3,3)	(0,4,3)	(1,4,3)	(0,2,1)	(0,1,2)	(0,4,3)	(4,4,3)
(2,0,3)	(0,1,3)	(0,2,3)	(0,4,3)	(1,3,3)	(0,2,1)	(0,2,2)	(0,3,3)	(1,4,3)
(0,2,1)	(0,1,3)	(0,1,3)	(0,4,3)	(1,4,3)	(0,2,3)	(0,1,3)	(0,4,3)	(2,4,3)
(1,0,3)	(0,2,1)	(0,2,3)	(0,4,3)	(0,4,3)	(0,2,0)	(0,4,3)	(0,3,3)	(4,4,3)
(0,1,3)	(0,2,3)	(0,1,3)	(0,4,3)	(0,2,3)	(0,2,3)	(0,2,3)	(0,4,3)	(2,4,3)
(0,1,1)	(0,1,1)	(0,2,1)	(0,3,3)	(1,2,3)	(0,2,1)	(0,1,2)	(0,3,3)	(3,4,3)
(0,0,1)	(0,1,2)	(0,2,2)	(0,4,3)	(0,4,3)	(0,2,1)	(0,2,1)	(0,4,3)	(4,4,3)

there are three hit points. Note that, when a tracker fails at each of the failure points, it will fail for the rest of the points, as well. As a result, having four failures for a tracker means that it has been a failure at the beginning of the tracking process. Taking the results given in Table 2, the designed tracker has an acceptable performance through the challenges mentioned in the first scenario. An important point here is that despite the cluttered background, the proposed tracker has performed well when dealing with similar environmental structures like billboards in the background. Besides, in the second scenario, the proposed tracker has performed the tracking successfully with no failures for %40 of the simulations while the others including the CNN based GOTURN tracker have failed at least one time in each simulation. This means that considering the challenges mentioned in the second scenario, one common failure among all the trackers except the proposed one is the short-term occlusion. Thus, as it has been claimed, the proposed tracker may even handle short-term occlusions. Finally, for the third scenario, the proposed tracker stands with 18 failures while the GOTURN as the other CNN based tracker has at least 23 failures indicating

that the designed tracker has significant advantages compared to the GOTURN tracker. In conclusion, the promising results of the designed tracker demonstrate some of its superiorities over the commonly employed trackers in the literature considering its acceptable performance through various challenging situations.

4.5. Performance of the Proposed Tracker on the LaSOT Dataset

In this part, as the final study of the proposed tracker performance, another dataset called LaSOT[21] is examined to train the proposed architecture on it. Furthermore, the tracker is compared to the state-of-the-art and recently proposed tracker called "SPLT" [30] to get better insight on the results. Although a complete comparison has been made on the commonly used trackers, performing this comparison may help to further demonstrate the proposed tracker capabilities. Furthermore, to avoid worries related to implementing this tracker on another dataset which may downgrade its performance, both trackers are trained on the LaSOT dataset where SPLT has been trained and tested on it.

The overview of SPLT tracker [30] is shown in Fig. 16, where the authors have claimed a robust and realtime performance on this structure. The SPLT tracker is based on the proposed skimming and perusal modules. Furthermore, a verifier based on ResNet50 is utilized to infer whether the object is absent or present. This outcome is employed to choose between performing a global search or a local one. The results given in [30] are very promising, indicating the SPLT tracker could be named as the state-of-the-art tracker in this field. Although by using strong hardware it may perform realtime, due to its heavy architecture, it is not comparable with our proposed tracker in terms of speed. Our running observation shows that this tracker is at least five time slower than that of our proposed tracker. Consequently, the comparison may challenge the proposed tracker accuracy, and not its speed. In this regard, considering the proposed tracker light structure, it is not expected to get higher accuracy. However, an acceptable performance compared to the SPLT may demonstrate its capabilities in both long-term tracking and other challenging situations. For this

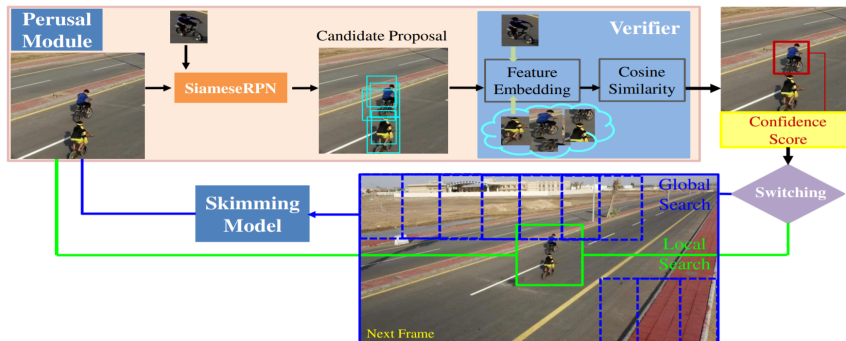


Figure 16: Skimming-Perusal’ long-term tracking framework presented by [30]

means, four scenarios are taken into account each having different challenges. These scenarios correspond to "airplane-9", "boat-4", "bottle-18", and "cat-1" test videos in LaSOT. The first two scenarios are considered as long-term tracking with various challenges such as short-term occlusion, diverse point of view, frequent change in the object size, different movement speed, and zooming in or out. The results of using the proposed tracker and the SPLT are shown in Fig. 17. In the first figure on the left side, an improper initialization is considered for the proposed tracker to further make it more challenging to continue on the tracking. Since the SPLT tracker could not handle the occlusion, it is tried to make the situation even harder for the proposed tracker to see if it can handle such situation. As it is seen in this figure, even though the IoU corresponding to the proposed tracker has been decreased to nearly a failure, it could properly handle the occlusion and enhance the IoU gradually, as it can be seen in Fig. 17 (a) from frame number 1000 to 2500. Here, an important note to ponder is that although the proposed tracker is much faster and it does not have a global searching module, it could properly handle a short-term occlusion, and it could maintain a constant IoU average over the whole tracking task. Fig. 17 (b) shows the results corresponding to a task of tracking a boat. In this task, challenges are similar to the previous one except that the camera has much higher movement compared to that of the previous task. Compared to the SPLT, the proposed tracker performs properly and in some situations even

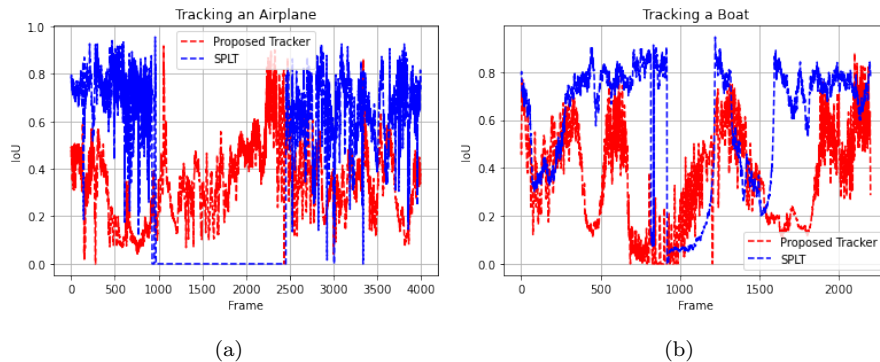


Figure 17: This figure illustrates the results of the proposed tracker and the SPLT on two long-term tracking scenarios.

better than that of the SPLT. The outstanding characteristic of the proposed tracker is that it can keep low IoU to a small amount without failure, and more importantly, it consistently improves the predictions without having a global search module.

The other two scenarios, on the other hand, contains blurry images caused by the camera rapid movements, abrupt change in the object position, and zooming in and out. Results are reported in Fig. 18. As it is seen in this figure, dealing with the challenges in these scenarios, the proposed tracker performed even better than the former two scenarios. Note that the improper initialization is considered deliberately as these cases as well, to examine the tracking task failure or downgrading in the performance. The aim of this type of initialization is to further demonstrate the tracker’s capability in enhancing the results. As shown in Fig. 18b by considering the results obtained in these two scenarios, the performance of the proposed tracker is comparable and even better than that of the SPLT results in terms of accuracy. Finally, our claim about handling short-term occlusions is verified by both the failure study and this comparison.

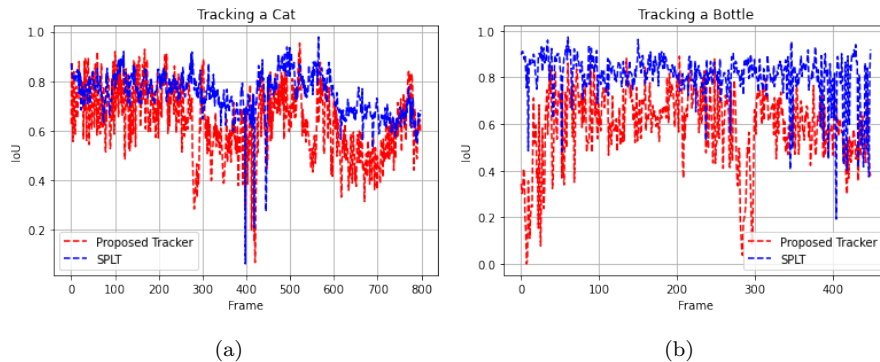


Figure 18: The first result corresponds to a video of a cat in which the cat sometimes changes its position suddenly while the camera zooms in or out. The other outcome reports the results of the two tracker on tracking an object while having severe fluctuations in the camera caused by its movement. This results in a completely blurred images and abrupt change in the object position.

5. Conclusions

In this paper, a training approach is presented to precisely localize the object in an image. The ROI and the center point matrices are used to determine the region of interest and the most probable center point of the object in the image, respectively. Furthermore, considering various input sizes, a single multiple-model CNN is proposed. This model contains a flexible structure with distinct and common layers to keep the performance high regardless of the object sizes. To demonstrate the capability of both the training method and the suggested model, a tracking application has been considered, and two comparative studies over eight OpenCV trackers including the GOTURN, and a recently proposed tracker called SPLT are performed. These studies reveal the applicability of the suggested tracker and the proposed training approach. Note that there are some limitations to the suggested method. For instance, the proposed approach does not distinguish between objects, and it has a part to extract distinct features. Moreover, even though the issues like short-term occlusion may be well handled compared to the other trackers, it is dispensable to have a specific module to

handle long-term occlusions where features may be lost. Consequently, our current research is focused on adding a classifier module in addition to a recurrent neural network module to address the above mentioned challenges.

References

References

- [1] W. Liu, D. Anguelov, D. Erhan, C. Szegedy, S. Reed, C.-Y. Fu, A. C. Berg, Ssd: Single shot multibox detector, in: European conference on computer vision, Springer, 2016, pp. 21–37.
- [2] T.-Y. Lin, P. Goyal, R. Girshick, K. He, P. Dollár, Focal loss for dense object detection, in: Proceedings of the IEEE international conference on computer vision, 2017, pp. 2980–2988.
- [3] J. Redmon, A. Farhadi, Yolov3: An incremental improvement, CoRR abs/1804.02767. [arXiv:1804.02767](https://arxiv.org/abs/1804.02767).
URL <http://arxiv.org/abs/1804.02767>
- [4] Y. LeCun, L. Bottou, Y. Bengio, P. Haffner, Gradient-based learning applied to document recognition, Proceedings of the IEEE 86 (11) (1998) 2278–2324.
- [5] A. Krizhevsky, I. Sutskever, G. E. Hinton, Imagenet classification with deep convolutional neural networks, in: Advances in neural information processing systems, 2012, pp. 1097–1105.
- [6] K. Simonyan, A. Zisserman, Very deep convolutional networks for large-scale image recognition, in: International Conference on Learning Representations, 2015.
- [7] C. Szegedy, W. Liu, Y. Jia, P. Sermanet, S. Reed, D. Anguelov, D. Erhan, V. Vanhoucke, A. Rabinovich, Going deeper with convolutions, in: Proceedings of the IEEE conference on computer vision and pattern recognition, 2015, pp. 1–9.

- [8] C. Szegedy, V. Vanhoucke, S. Ioffe, J. Shlens, Z. Wojna, Rethinking the inception architecture for computer vision, in: Proceedings of the IEEE conference on computer vision and pattern recognition, 2016, pp. 2818–2826.
- [9] R. Girshick, J. Donahue, T. Darrell, J. Malik, Rich feature hierarchies for accurate object detection and semantic segmentation, in: Proceedings of the IEEE conference on computer vision and pattern recognition, 2014, pp. 580–587.
- [10] J. R. Uijlings, K. E. Van De Sande, T. Gevers, A. W. Smeulders, Selective search for object recognition, *International journal of computer vision* 104 (2) (2013) 154–171.
- [11] K. He, X. Zhang, S. Ren, J. Sun, Spatial pyramid pooling in deep convolutional networks for visual recognition, *IEEE transactions on pattern analysis and machine intelligence* 37 (9) (2015) 1904–1916.
- [12] R. Girshick, Fast r-cnn, in: Proceedings of the IEEE international conference on computer vision, 2015, pp. 1440–1448.
- [13] S. Ren, K. He, R. Girshick, J. Sun, Faster r-cnn: Towards real-time object detection with region proposal networks, in: *Advances in neural information processing systems*, 2015, pp. 91–99.
- [14] T.-Y. Lin, M. Maire, S. Belongie, J. Hays, P. Perona, D. Ramanan, P. Dollár, C. L. Zitnick, Microsoft coco: Common objects in context, in: *European conference on computer vision*, Springer, 2014, pp. 740–755.
- [15] R. Caruana, Multitask learning, *Machine learning* 28 (1) (1997) 41–75.
- [16] A. Pentina, V. Sharmanska, C. H. Lampert, Curriculum learning of multiple tasks, in: *Proceedings of the IEEE Conference on Computer Vision and Pattern Recognition*, 2015, pp. 5492–5500.

- [17] S. Bell, C. Lawrence Zitnick, K. Bala, R. Girshick, Inside-outside net: Detecting objects in context with skip pooling and recurrent neural networks, in: Proceedings of the IEEE conference on computer vision and pattern recognition, 2016, pp. 2874–2883.
- [18] G. Bradski, The OpenCV Library, Dr. Dobb’s Journal of Software Tools.
- [19] K. He, G. Gkioxari, P. Dollár, R. Girshick, Mask r-cnn, in: Proceedings of the IEEE international conference on computer vision, 2017, pp. 2961–2969.
- [20] H. K. Galoogahi, A. Fagg, C. Huang, D. Ramanan, S. Lucey, Need for speed: A benchmark for higher frame rate object tracking, CoRR abs/1703.05884. [arXiv:1703.05884](https://arxiv.org/abs/1703.05884).
URL <http://arxiv.org/abs/1703.05884>
- [21] H. Fan, H. Bai, L. Lin, F. Yang, P. Chu, G. Deng, S. Yu, M. Huang, J. Liu, Y. Xu, et al., Lasot: A high-quality large-scale single object tracking benchmark, International Journal of Computer Vision (2020) 1–23.
- [22] H. Grabner, H. Bischof, On-line boosting and vision, in: 2006 IEEE Computer Society Conference on Computer Vision and Pattern Recognition (CVPR’06), Vol. 1, Ieee, 2006, pp. 260–267.
- [23] B. Babenko, M.-H. Yang, S. Belongie, Visual tracking with online multiple instance learning, in: 2009 IEEE conference on computer vision and pattern recognition, IEEE, 2009, pp. 983–990.
- [24] J. F. Henriques, R. Caseiro, P. Martins, J. Batista, High-speed tracking with kernelized correlation filters, IEEE transactions on pattern analysis and machine intelligence 37 (3) (2014) 583–596.
- [25] A. Lukezic, T. Vojir, L. Cehovin Zajc, J. Matas, M. Kristan, Discriminative correlation filter with channel and spatial reliability, in: Proceedings of the IEEE Conference on Computer Vision and Pattern Recognition, 2017, pp. 6309–6318.

- [26] Z. Kalal, K. Mikolajczyk, J. Matas, Forward-backward error: Automatic detection of tracking failures, in: 2010 20th International Conference on Pattern Recognition, IEEE, 2010, pp. 2756–2759.
- [27] Z. Kalal, K. Mikolajczyk, J. Matas, Tracking-learning-detection, IEEE transactions on pattern analysis and machine intelligence 34 (7) (2011) 1409–1422.
- [28] D. S. Bolme, J. R. Beveridge, B. A. Draper, Y. M. Lui, Visual object tracking using adaptive correlation filters, in: 2010 IEEE computer society conference on computer vision and pattern recognition, IEEE, 2010, pp. 2544–2550.
- [29] D. Held, S. Thrun, S. Savarese, Learning to track at 100 fps with deep regression networks, in: European Conference on Computer Vision, Springer, 2016, pp. 749–765.
- [30] B. Yan, H. Zhao, D. Wang, H. Lu, X. Yang, 'skimming-perusal'tracking: A framework for real-time and robust long-term tracking, in: Proceedings of the IEEE International Conference on Computer Vision, 2019, pp. 2385–2393.